The H-mode density limit in the full tungsten ASDEX Upgrade tokamak

M. Bernert[1], T. Eich[1], A. Kallenbach[1], D. Carralero[1], A. Huber[2], P.T. Lang[1], S. Potzel[1], F. Reimold[1], J. Schweinzer[1], E. Viezzer[1], H. Zohm[1] and the ASDEX Upgrade team
[1] *Max Planck Institute for Plasma Physics, Boltzmannstr. 2, 85748 Garching, Germany and*
[2] *Forschungszentrum Juelich GmbH, 52425 Juelich, Germany*

The high confinement mode (H-mode) is the operational scenario foreseen for ITER, DEMO and future fusion power plants. At high densities, which are favorable in order to maximize the fusion power, a back transition from the H-mode to the low confinement mode (L-mode) is observed. In present tokamaks, this H-mode density limit (HDL) occurs at densities on the order of, but below, the Greenwald density.

In gas ramp discharges at the fully tungsten covered ASDEX Upgrade tokamak (AUG), four distinct operational phases are identified in the approach towards the HDL. These phases are a stable H-mode, a degrading H-mode, the breakdown of the H-mode and an L-mode. They are reproducible, quasi-stable plasma regimes and provide a framework in which the HDL can be further analyzed. During the evolution, energy losses are increased and a fueling limit is encountered. The latter is correlated to a plateau of electron density in the scrape-off layer (SOL). The well-known extension of the good confinement at high density with high triangularity is reflected in this scheme by extending the first phase to higher densities.

In this work, two mechanisms are proposed, which can explain the experimental observations. The fueling limit is most likely correlated to an outward shift of the ionization profile. The additional energy loss channel is presumably linked to a regime of increased radial filament transport in the SOL. The SOL and divertor plasmas play a key role for both mechanisms, in line with the previous hypothesis that the HDL is edge-determined.

The four phases are also observed in carbon covered AUG, although the HDL density exhibits a different dependency on the heating power and plasma current. This can be attributed to a changed energy loss channel in the presented scheme.

I. INTRODUCTION

For a sufficient energy production and fusion performance, DEMO and future fusion power plants are foreseen to operate at highest densities in the high confinement mode (H-mode)[3–7]. The H-mode operation is accessed by applying sufficient heating power to the plasma[2,3]. However, the operation of a tokamak at high densities is limited by the so-called Greenwald limit[12,13]

$$n_{GW} = \frac{I_p}{\pi a^2},$$

where n_{GW} is the line averaged density in units of $10^{20}\,\mathrm{m}^{-3}$, I_p the plasma current in MA and a the minor radius in m. At Greenwald fractions ($f_{GW} = \frac{\overline{n}_e}{n_{GW}}$) of about 0.8-1.2, the plasma is observed to end in a disruption. Therefore, the Greenwald limit represents a hard limit.

At high densities also a back transition from the H-mode to the low confinement mode (L-mode) is observed. This H-mode density limit (HDL) typically takes place at Greenwald fractions of 0.8-1[12]. The HDL represents a soft limit, as the plasma operation can be continued at the lower confinement and a renewed transition into H-mode is in principle possible. In typical gas ramp discharges, the density increases further after the HDL until the Greenwald limit is reached.

Both the Greenwald limit and the HDL can be exceeded by centrally elevated density profiles, as they are achieved in todays experiments by pellet fueling[20].

This paper focuses on the characterization of the H-mode density limit by a classification of the different sequences of temporal evolution of the plasma edge parameters and gives an initial interpretation of the observed effects.

The HDL has to be discriminated against an H-L transition, which is caused by the reduction of the heating power below the threshold, since it is reported to be independent of the heating power[15,25].

Studies at ASDEX Upgrade (AUG) and JET, both with a fully carbon covered wall, attribute the HDL to the full detachment of the divertor[5,7]. In these studies, the H-L back transition is linked to a radiation instability close to or inside the confined region of the plasma, which is triggered by the detachment.

At AUG and JET, the first wall material was changed to tungsten and tungsten and beryllium, respectively, which has a significant impact on the radiation characteristics of the plasma. Therefore, the HDL is investigated in the presented work at the fully tungsten covered ASDEX Upgrade (full-W AUG).

This paper is organized as follows. The performed experiments and their gas fueling schemes are described in Section II. The four phases, which are identified in the approach towards the HDL, are introduced and characterized in Section III. Several mechanisms, which were previously proposed to cause the HDL, are examined in full-W AUG in Section IV. A regression analysis of the maximum achieved densities in H-mode is given in Section V. A new interpretation of the HDL, based on the observation of the four phases, and related mechanisms

are proposed in Section VI. The impact of centrally elevated density profiles investigated in Section VII and the presented work is summarized in Section VIII.

II. EXPERIMENTS

A. Discharge setup

Between 2011 and 2014 over 30 dedicated gas ramp discharges were conducted at AUG in order to study the HDL in a full-W tokamak. The standard scenario for these studies is a gas ramp discharge with a plasma current of I_p = 0.8 MA, a toroidal magnetic field on-axis of B_t = -2.5 T and hence a safety factor q_{95} of about 6. The averaged triangularity is in the low to medium range of $\delta_{av} \approx 0.23$. The discharges are heated by neutral beam injection (NBI) with a standard input power of P_{heat} = 7.5 MW, which is well above the L-H power threshold of about 3.3 MW (at a separatrix surface of 43.6 m^2).

The magnetic equilibrium of the standard scenario and the location of the main measurements can be seen in Figure 1. The electron density measured by interferometry is given throughout this publication in line integrated rather than line averaged measurements. This is necessary due to a significant electron density in the scrape-off layer (see Fig. 9a & 10), which would otherwise be erroneously interpreted as density within the confined region. For an estimation of the line averaged densities, a chord length of the central chord (H-1) of 1.02 ± 0.03 m and of the edge chord (H-5) of 0.79 ± 0.02 m can be used, which are (within the error bars) the same for all presented discharges of full-W AUG.

The dataset of 30 discharges contains separate scans of safety factor, plasma current, external heating power and triangularity, which are discussed in Section V.

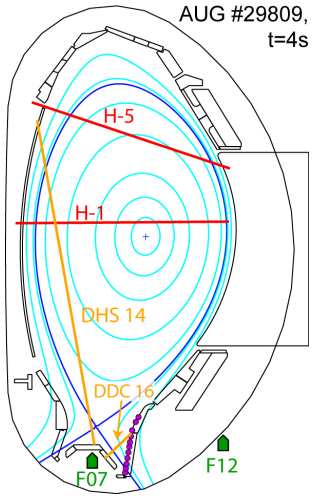

Figure 1. Magnetic equilibrium (blue, cyan) of an HDL discharge and the location of the main measurements used in the presented work: edge (H-5) and core (H-1) interferometry (red), ionisation gauges (green), Langmuir probes in the outer divertor (purple) and two lines of sight of the AXUV diode system (orange).

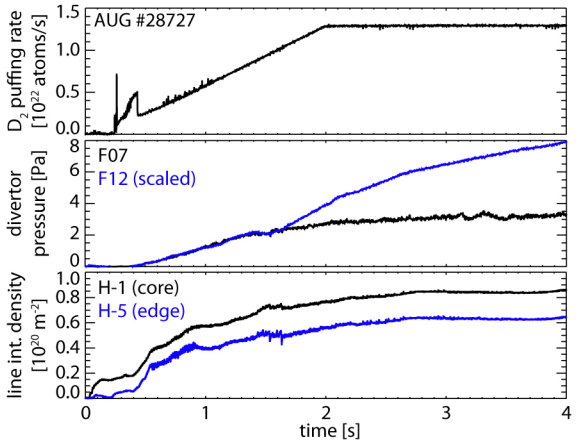

Figure 2. Typical time traces of neutral gas fueling rate, neutral gas pressure in the divertor measured by ionization gauges and line integrated electron density of an HDL discharge. The ionization gauge below the roof baffle (F07) saturates at around 1.6 s, the neutral gas pressure can be estimated out of the measurements of a gauge situated in the pump chamber (F12), which is scaled to match the unsaturated measurement below the roof baffle.

B. High density operation and fueling

The HDL discharges are only fueled externally by valves in the private flux region of the lower divertor, fueling by the NBI is negligible. A neutral pressure in the divertor of up to 8 Pa is necessary to achieve the plasma densities relevant for the HDL. AUG has to be operated solely with the turbo pump system and without the cryo pump system, reducing the pumping capacity by a factor of 8, in order to achieve these high pressures.

Figure 2 shows the gas fueling scheme for a typical HDL discharge. Due to the reduced pumping, the constant gas puff leads to a monotonic increase of the divertor neutral gas pressure.

A neutral gas pressure of several Pa is necessary for the HDL discharges since a fueling limit is reached. The fueling limit corresponds to a saturation of the plasma density relative to the neutral gas pressure in the divertor. In Figure 3 the electron density is plotted versus the neutral pressure. At low densities, the two measurements are almost proportional to each other (typical operational range, indicated by the green line). At medium to high densities, this relation becomes non-linear and a much higher divertor pressure is needed to achieve the same increase of plasma density (orange line). When the fueling limit is finally reached, the plasma density does not increase despite an increase of the neutral gas pressure by 30% (red line).

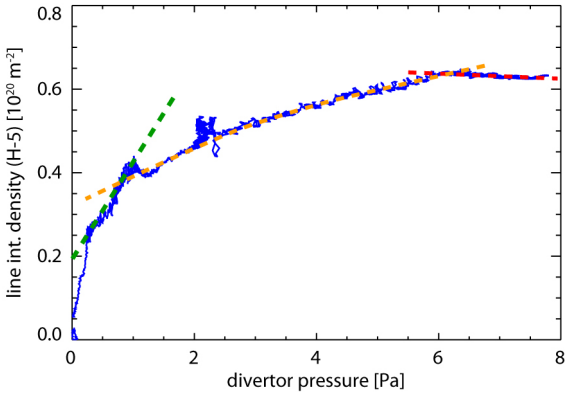

Figure 3. Line integrated edge density plotted versus the neutral gas pressure in the divertor as shown in Figure 2. The plasma density saturates and reaches a fueling limit (red line).

C. Evolution of a typical HDL gas ramp discharge

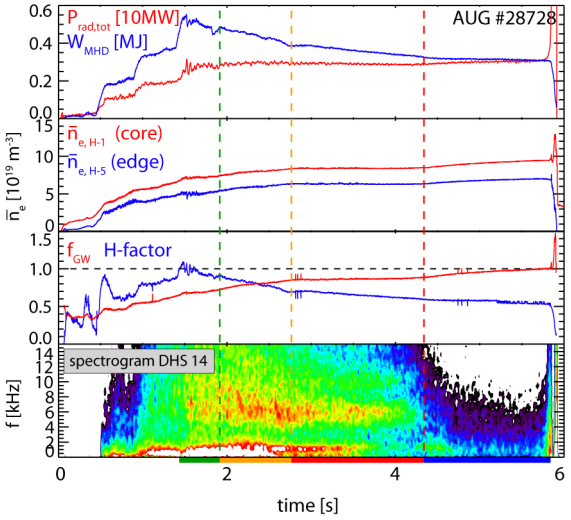

Figure 4. Time traces of radiated power and stored energy, edge and central line integrated electron density, Greenwald fraction and H-factor and a spectrogram of an AXUV diode signal observing the X-point of HDL discharge AUG #28728. The colored bars on bottom indicate the four phases discussed in Section III.

Figure 4 shows several time traces of a typical HDL gas ramp discharge. The ramp-up of plasma shape, current and heating power is finished at 1.5 s. From this point on, all external parameters are kept constant except the neutral gas pressure, which is increased by the constant gas puff (similar to Fig. 2).

The plasma stored energy decreases constantly, indicating a reduction of the energy confinement time. This can also be observed in the reduction of the H-factor, which gives the energy confinement time with respect to the ITERH98P(y,2) scaling[27]. The total radiated power, determined out of bolometry measurements[4,11], is constant or even slightly reducing during the discharge up to the disruption. Due to the high gas puff is the tungsten concentration in general below $5 \cdot 10^{-5}$ (in most cases below $1 \cdot 10^{-5}$) for the HDL discharges and has no significant effect on the plasma radiation.

The transition from type-I to type-III edge localized modes (ELMs), which is typically observed at high densities[34,38], takes place in the presented discharge between 1.5 and 1.7 s. The spectrogram of an AXUV diode channel[4] observing the X-point shows a broad frequency band around 6 kHz. This is characteristic for the X-point fluctuations, which are not specific to the H-mode and are most likely correlated with the regime of divertor detachment[29]. The full detachment of the outer divertor, which is for full-C AUG reported to trigger the HDL[7], takes place immediately before the disruption, here at around 5.8 s. The full detachment is correlated with the development of a MARFE[21] at the X-point, which subsequently moves upwards. Along with this movement a tearing mode (typically 2-1) is triggered, which finally causes the disruption, resembling the "Greenwald-like" L-mode density limit.

III. THE FOUR PHASES OF THE H-MODE DENSITY LIMIT

In the gas ramp discharges at AUG, four distinct phases are identified in the approach towards the HDL. These phases are distinguished by their impact on the plasma stored energy (W_{MHD}) and the edge line integrated electron density ($\overline{n}_{e,H-5}$). In Figure 5 these two parameters are plotted against each other, highlighting the different phases. The four phases are identified as:

1. A stable H-mode,
2. a degrading H-mode,
3. the breakdown of H-mode and
4. an L-mode.

The phases can also be distinguished by their impact on the pedestal top temperature, as shown in Figure 6b. The first phase evolves along an isobaric line, while in the second and third phases the pressure reduces, and thus the confinement degrades.

The four phases are observed in all discharges dedicated to the HDL studies at full-W AUG, independent of the discharge parameters and fueling approaches. However, the timing and duration of the phases change significantly. Figure 7 shows the $W_{MHD} - \overline{n}_{e,H-5}$ plots for various discharge parameters in full-W AUG, all exhibiting similar characteristics. The same observation can be made for the HDL discharges in full-C AUG, as seen in Figure 8.

The instantaneous change of the plasma behaviour (specifically, the change of the stored energy relative to the density increase, as seen in Fig. 5-8) at the transition from one phase to another indicates that the individual

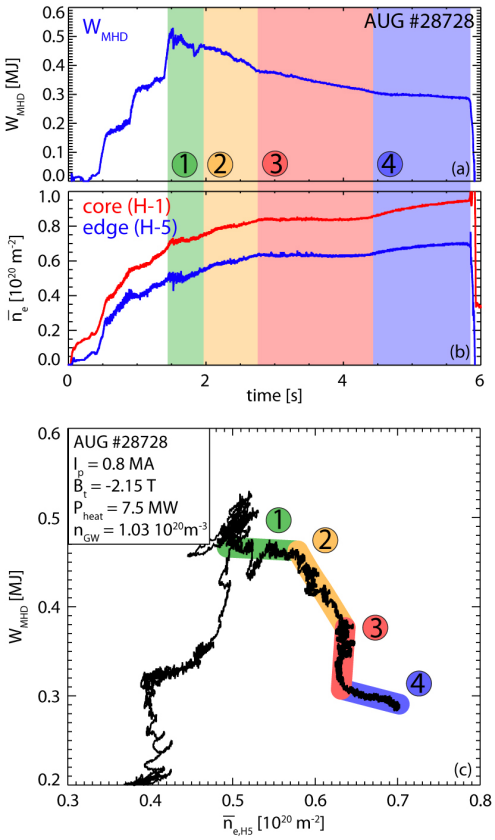

Figure 5. a,b: Time traces of stored energy and line integrated density of HDL discharge AUG #28728. The background colors indicate the time duration of the four phases identified in Figure c.
c: Stored energy plotted versus edge line integrated density.

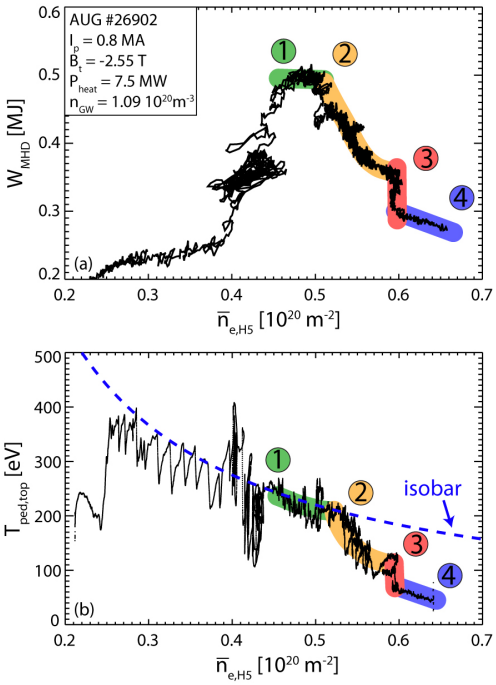

Figure 6. a: $W_{MHD} - \overline{n}_{e,H-5}$ plot for HDL discharge AUG #26902. b: Estimate of the pedestal top temperature plotted versus the edge density. The four phases can also be distinguished, the first phase evolves along an isobaric line. The strong oscillations are caused by heating steps and ELMs.

phases are discrete plasma states. This instantaneous change can also be seen in the change of gradients of the time traces shown in Figure 4 & 5(a,b).

Every phase can be accessed directly (e.g. by an increase of heating power, seen in Fig. 7c-d) and is stable against ELMs or short trips of heating power. This indicates, that the four phases are reproducible, discrete and quasi-stable plasma regimes, which are present independent of the first wall material and discharge parameters, and, thus, characteristic for the high density operation at AUG. They provide a framework in which the HDL can be further analyzed.

The characteristics of the phases and their impact on the electron density and temperature profiles (see Fig. 9) are listed in the following:

1 The **stable H-mode** is the standard operational H-mode regime: the plasma density increases at a stable confinement. The pressure is constant and the plasma evolves along an isobaric line (see Fig. 6). The increase in electron density takes place in the plasma core and edge and, since the pressure is constant, the electron temperature decreases accordingly.

The transition from type-I to type-III ELMs takes place typically, but not exclusively, in this phase.

2 In the second phase, the **degrading H-mode**, the confinement reduces, corresponding to a loss of pressure. The electron density in the confined region stays almost constant while a plateau of electron density evolves in the scrape-off layer (SOL) up to about 40-50% of the pedestal top density. Meanwhile, the width of the temperature pedestal reduces, leading to a lower pedestal top and central electron temperature (see Fig. 9).

3 The third phase, the **breakdown of the H-mode**, is characterized by an overall fixed radial electron density profile. Measurements of the electron density by the Li-beam and Thomson Scattering diagnostics during this phase are compared in Figure 10.

The confinement keeps decreasing at constant density, which leads to the step-like function in the $W_{MHD} - \overline{n}_{e,H-5}$ plot. The gradient of the electron temperature in the pedestal is also constantly decreasing during this phase, which leads to a reduced temperature and pressure in the confined region and, thus, to the reduction of confinement. Along with the electron temperature gradient, also the radial electric field (E_r) well depth at the pedestal is continuously decreasing up to about -15 kV/m (see Sec. IV). The whole phase is still defined as an H-mode, since ELMs exist and E_r stays below the reported threshold of -15 kV/m[32] up to the end of this phase.

The duration of breakdown phase varies between 0.1 s and 4 s. Therefore, it also resembles a quasi-stable

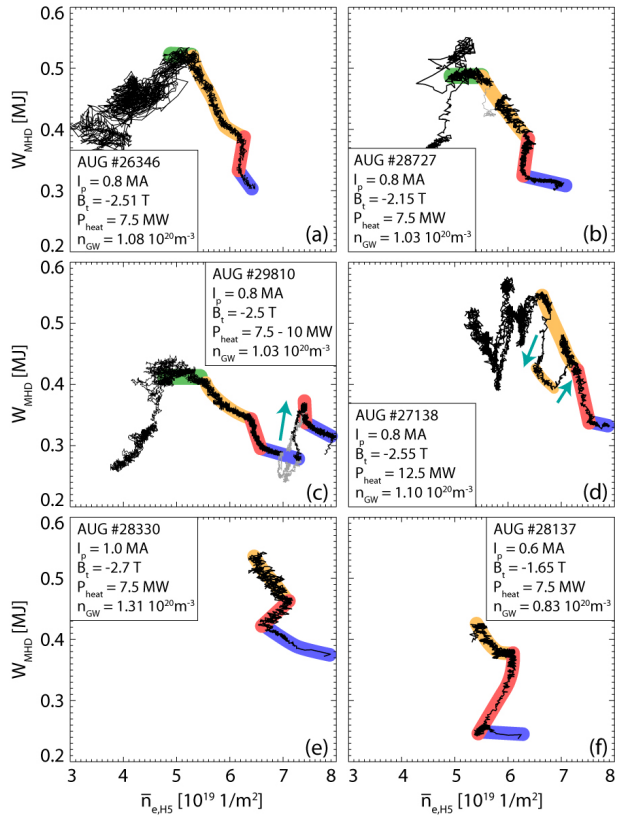

Figure 7. $W_{MHD} - \overline{n}_{e,H-5}$ plots of various HDL discharges in full-W AUG. Trips of heating power are shaded in grey, NBI heating steps ($\Delta P_{heat} = 2.5\,\mathrm{MW}$) indicated by cyan arrows. The four phases are always reproduced, quasi-stable and can directly be accessed e.g. by heating steps as seen in Figures c and d.

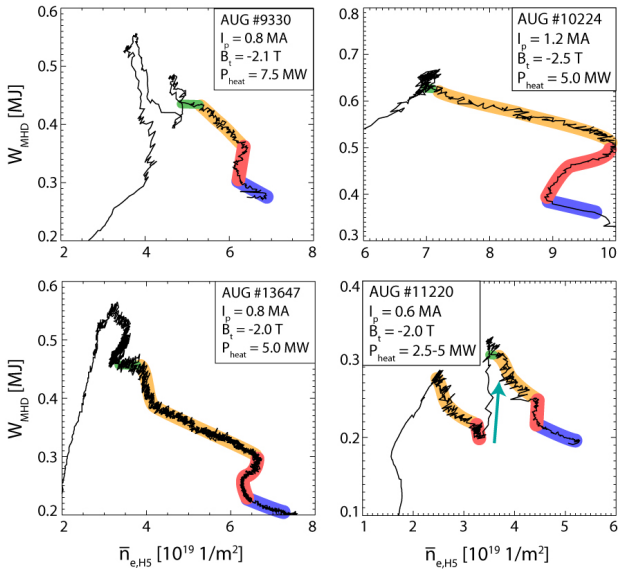

Figure 8. $W_{MHD} - \overline{n}_{e,H-5}$ plots of various HDL discharges in full-C AUG. The four phases are also observed with the different first wall material.

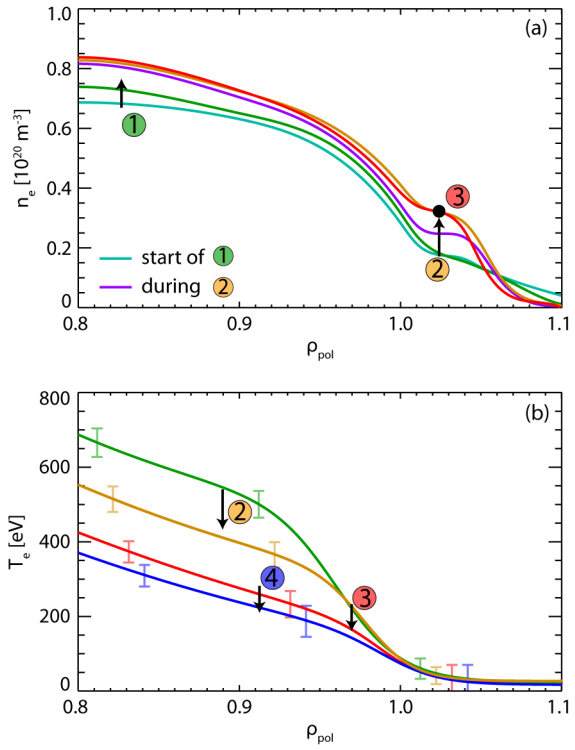

Figure 9. Radial profiles of electron density (a, AUG #28726, fitted to data from the interferometry, Thomson scattering and Lithium beam diagnostics, details shown in Fig. 10) and electron temperature (b, AUG #29809, fitted to data from the ECE and Thomson scattering diagnostics) at the end of the corresponding phases. The arrows and numbers indicate the radial position and the phase in which the predominant changes in the profiles occur.

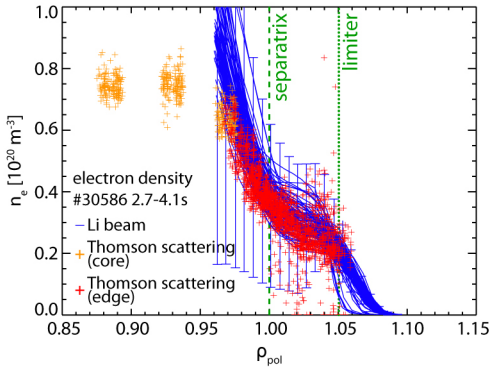

Figure 10. Electron density measurements during the breakdown phase of HDL discharge AUG #30586. The profile does not change during the whole phase.

plasma regime. This phase is here defined as the actual H-mode density limit, since it resembles the H-mode with the highest edge density, and used for the regression analysis in Section V. However, all four phases have to be regarded in order to find an explanation for the HDL.

4 The last phase resembles an **L-mode** with a typi-

cal H-factor of about 0.5. The confinement stays almost constant in this phase and the plasma density increases again. During this phase, the outer divertor fully detaches and a MARFE evolves at the X-point. With the increasing density the L-mode density limit is reached, the MARFE moves upwards and a tearing mode is triggered, which finally leads to the disruption.

IV. PREVIOUSLY PROPOSED MECHANISMS FOR THE HDL

In previous studies several mechanisms were proposed to cause the HDL. These mechanisms are revised with the new database of full-W AUG, using the improved diagnostic capabilities.

A. Detachment

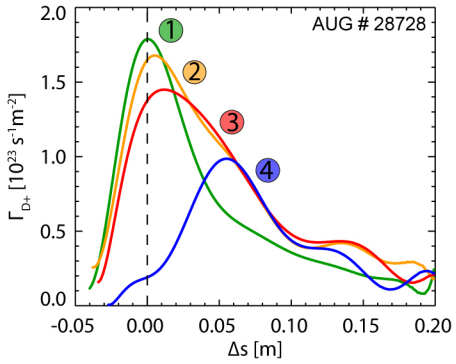

Figure 11. Averaged profiles of ion flux density to the divertor target plates for the different phases.

Full detachment of the outer divertor and related radiation losses were identified to trigger the HDL in full-C AUG[6]. In full-W AUG, the roll-over of the ion saturation current measurements at the outer strikeline starts during the breakdown of the H-mode and the outer divertor is in the L-mode phase in a partially detached regime. Full detachment is only achieved shortly before the disruption. The evolution of the ion flux density profiles for the different phases is shown in Figure 11. Note, that the high frequency ELMs during the second and third phase also affect the divertor condition.

In addition, stable H-modes are established in full-W AUG, which are fully detached during the inter-ELM phases[30]. Therefore, the full detachment can be refuted as a cause for the HDL in full-W AUG. However, it might play a significant role in the HDL of full-C AUG.

B. Radiation and MARFEs

Radiation in the confined plasma can increase the energy losses, reduce the power flux over the separatrix and lead to a back transition into L-mode. Also MARFEs, which evolve in full-W AUG typically in the X-point region, lead to such an increased radiation. In plasmas with a high impurity content, MARFEs are observed to trigger an H-L back transition by radiative cooling of the pedestal. However, in the dedicated HDL discharges, which have a low impurity concentration due to the high deuterium gas puff, the MARFE does not start evolving before the L-mode phase and, thus, is not related to the HDL.

Furthermore, the poloidal radiation distribution (see Fig. 12) and the total radiated power (see Fig. 4 & 17) stay constant (or even decreases) during the first three phases of the HDL discharges at full-W AUG. Therefore, in full-W AUG, no additional energy losses from the confined region are created by radiation.

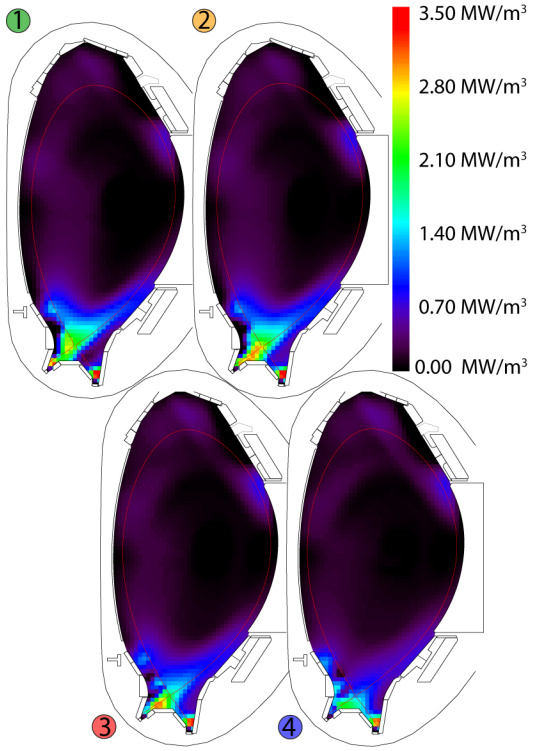

Figure 12. Deconvolution of the poloidal radiation distribution measured by bolometry for the four phases in AUG #29809. The radiation stays constant (or even decreases) throughout the discharge.

C. ELMs

ELMs are discussed in references[7,12] to trigger the HDL: The pedestal might be more eroded by high frequency ELMs than can be recovered in the short inter-ELM phase.

The ELM frequency increases in full-W AUG strongly when approaching the HDL, but also the ELM size (relative loss of stored energy per ELM, also seen in the ELM-

induced radiation, Figure 13) reduces. While the degradation of the confinement and, thus, the energy losses are ongoing the ELMs are occasionally observed to vanish during the breakdown of the H-mode (see Figure 13 and in the low frequency range of the bottom plot of Fig. 4). Therefore, there must be another effect leading to the energy loss.

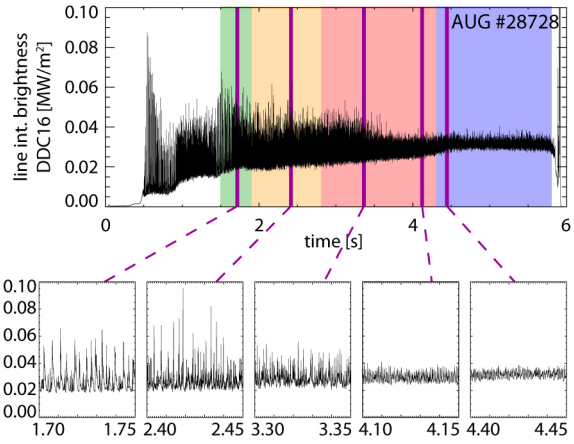

Figure 13. Measurement of an AXUV channel observing the outer divertor. The ELMs vanish during the third phase (third and fourth bottom plots), only small high frequent fluctuations remain, which are also present in the L-mode phase.

Furthermore, the transition from type-I to type-III ELMs (not shown here) is not related to any of the HDL phases and is observed to take place in the first or in the third phase.

D. Thresholds of heating power and radial electric field

H-L back transitions take place if the heating power is reduced below the L-H power threshold (taking also into account the L-H-L hysteresis).

For the HDL discharges in full-W AUG, the divertor loss power is significantly above the L-H power threshold scaling ($P_{L-H} \approx 3.3\,\mathrm{MW}$,[23]) during the first three phases. The divertor loss power is the sum of the power radiated in the divertor volume, measured by bolometry, and the power deposited on the target plates, measured by thermography, and must be lower or equal to the power flowing over the separatrix. Therefore, additional energy losses from the confined region do not reduce the power flux over the separatrix below the reported threshold. However, the threshold might be important for the final transition from the breakdown phase of the H-mode to the L-mode, where the divertor loss power is close to the threshold.

In reference[32] a threshold for the depth of the radial electric field (E_r) well in the pedestal of -15 kV/m is reported for the L- to H-mode transition at similar discharge parameters. Figure 14 shows the evolution of the diamagnetic term of the radial force balance, which is an

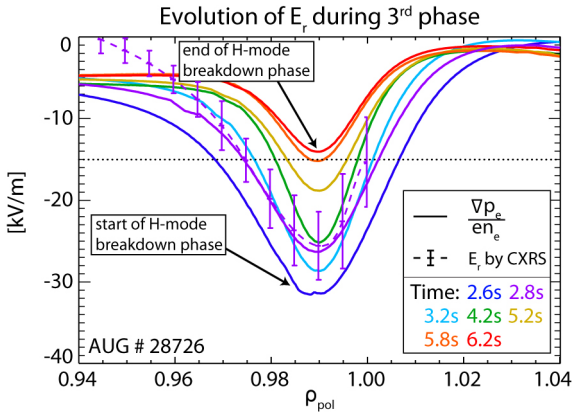

Figure 14. Measurement of the radial electric field (dashed line) and evolution of an estimate for the radial electric field well during the breakdown phase of the H-mode in AUG #28726. The reported threshold[32] is indicated by the dotted line.

estimate of E_r ($E_r \approx \frac{\nabla p_i}{e n_i} \approx \frac{\nabla p_e}{e n_e}$,[35]), during the breakdown phase of the H-mode. At the onset of this phase, the E_r well is significantly below the threshold, as also seen by direct E_r measurements using charge exchange recombination spectroscopy (CXRS)[36]. Only at the end of this phase, the E_r well is close to the threshold. Therefore, the E_r is not related to the onset of the HDL, but might play a significant role at the final transition to L-mode.

It is seen that the threshold for the E_r well depth and for the heating power behave similar at the HDL of full-W AUG. Both might be determined by the same effect. The E_r threshold might also be interpreted as the local parameter which is described by the global L-H power threshold.

V. REGRESSION ANALYSIS

The onset of the different phases of the HDL could yet not be assigned to a fixed value of a specific parameter, such as temperature, plasma density or neutral gas pressure. In order to identify the parameter dependencies of the HDL, the 30 conducted discharges include separate scans of

- heating power ($6\,\mathrm{MW} \leq P_{heat} \leq 12.5\,\mathrm{MW}$),
- safety factor ($3.5 \leq q_{95} \leq 6$),
- plasma current ($0.6\,\mathrm{MA} \leq I_p \leq 1.2\,\mathrm{MA}$),
- toroidal magnetic field ($1.45\,\mathrm{T} \leq B_t \leq 2.7\,\mathrm{T}$) and
- triangularity ($0.23 \leq \delta \leq 0.37$).

A regression analysis of the achieved line integrated edge density ($\overline{n}_{e,H-5}$ in $10^{20}\mathrm{m}^{-2}$) at the onset third phase is performed. This represents the highest achieved pedestal top density in H-mode and, thus, a physical limit. The onset of the degrading H-mode phase, which might be more important as operational point of future

reactors, is not regressed here and subject to future studies.

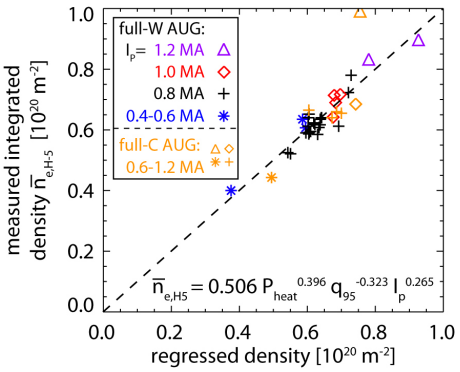

Figure 15. Regressed versus measured density at the onset of the third HDL phase, also including discharges of full-C AUG (orange), which were not included in the regression analysis.

The log-linear regression results in:

$$\overline{n}_{e,H5,regr.} = 0.506 \pm 0.192 \frac{P_{heat}^{0.396\pm0.13}\, I_p^{0.265\pm0.14}}{q_{95}^{0.323\pm0.14}}, \quad (1)$$

where the regression values are given with their 95% confidence intervals. The standard deviation is $\sigma = 0.0311$, regressed versus measured densities are shown in Figure 15.

The regression of the line integrated edge density ($\overline{n}_{e,H-5}$) leads to a more accurate result than the regression of the line averaged central density ($\langle n_{e,H-1}\rangle$, $\sigma_{H-1} = 0.058$). The scaling factor between the two values is around $\frac{\overline{n}_{e,H-5}}{\langle n_{e,H-1}\rangle} = 0.78 \pm 0.05\,\mathrm{m}$ for these flat density profiles. Note, however, that the density plateau in the SOL does lead to a wrong interpretation of the line averaged density (see Sec. II A).

Any combination of two parameters out of I_p, B_t and q_{95} can be used in the regression and leads to a similar fit quality due to the collinearity of the three parameters. The normalized pressure β_N does not lead to a better regression than the heating power P_{heat}. The triangularity does not have an effect on the density of the third phase and thus is omitted in the regression.

All dependencies in Equation 1 were reproduced in separate scans of the given parameters. Notably, the pronounced heating power dependence, which is for full-C AUG and JET reported to be not existent or insignificant[6,12,15,24], is seen within a discharge: In discharge AUG #29810, shown in Figure 7c, the heating power was increased in the fourth phase, which lead to a transition back into the breakdown phase of the H-mode at a higher density. This demonstrates directly to power dependence of the HDL.

The regression yields a significantly lower dependence on the plasma current than the Greenwald limit[13]. The empirical scaling of full-C AUG and JET[6] deviates from the above given regression in the dependence from the heating power and the plasma current as well as the triangularity. A more detailed comparison of these scalings is given in reference[3].

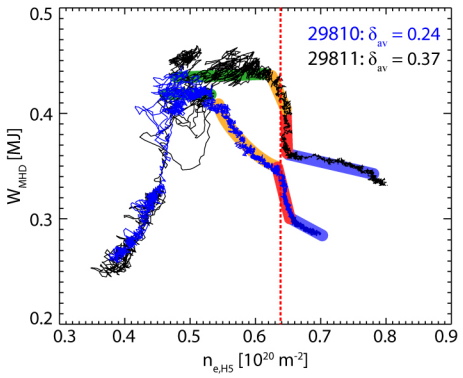

Figure 16. $W_{MHD} - \overline{n}_{e,H-5}$ plots for two discharges at different triangularities. The breakdown of the H-mode takes place at the same density, while the onset of the degradation is at a higher density for higher triangularity.

A variation of the triangularity reveals, that the density of the breakdown of the H-mode is not depending on the triangularity. However, Figure 16 shows, that the onset of the degrading H-mode phase is at a higher density for the higher triangularity, i.e. the stable H-mode phase extends to higher densities. This is in line with the observations in references[31,33], which report no influence of the triangularity on the confinement for low densities, but a significant increase with triangularity at high densities. There is a contradiction with observations at the DIII-D tokamak[28]. There, a reduction of the pressure is seen with increasing density, similar to the degrading H-mode phase. However, the density, at which this reduction sets in, is at DIII-D independent of the triangularity (Fig. 4 of Re.[28]).

VI. INTERPRETATION OF THE FOUR PHASES

All mechanisms discussed in Section IV can be refuted as a cause for the HDL in full-W AUG. Instead, the observation of the four phases, described in Section III, provides a framework for a new interpretation of the underlying mechanisms of the HDL.

The influence of the phases on the plasma density and the stored energy has to be considered:

phase	plasma energy	plasma density
1	constant	increases
2	decreases	constant inside sep.
3	decreases	constant
4	constant	increases

The first and last phases are comparable to standard operation in H- or L-mode, respectively. The second

and third phase exhibit an increased energy loss and a non-linear density evolution. The observation of the four phases is caused by a coupling of these two effects.

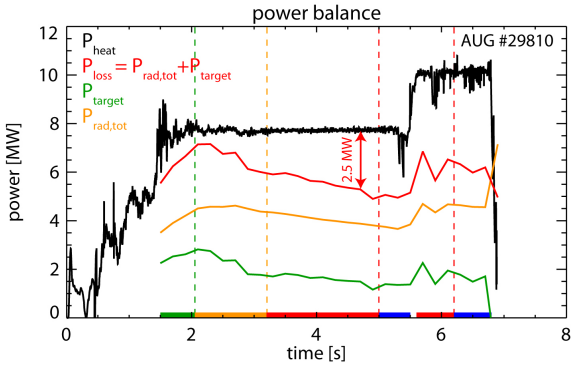

Figure 17. Time traces of the global power balance during HDL discharge AUG #29810: Total heating power (black), total loss power (red), power deposited on the divertor target plates (green) and total radiated power (orange). The four phases are indicated by the colored bars on the bottom.

The increased energy losses are evident in the global power balance of the plasma, shown in Figure 17. The power balance compares the total heating power (NBI and ohmic) with the sum of the power deposited on the divertor target plates and the total radiated power. In the first phase the heating power is matched to about 90%, the expected value for standard operation in H-mode[14]. During the second to fourth phase, the power balance shows a significant mismatch of up to 3MW, corresponding to almost 40% of the heating power. This is significantly higher than the neutral beam losses ouside the confined plasma, which are estimated to be below 1 MW. The missing power is neither radiated nor deposited on the divertor target plates. Therefore, a significant part of this power must be transported to the main chamber walls. To prove the latter, a direct measurement of the heat deposition on the first wall is in preparation.

The mismatch of the power balance indicates that an additional energy loss channel opens up. Such a high power deposition on the first wall might be caused by a regime of increased radial filament velocity in the SOL[9,26], which increases the radial SOL transport significantly. This regime, which is observed for high densities at AUG[8], JET[9] and Alcator C-mod[18], is depending on the collisionality[26] along the magnetic field lines and is most likely triggered by the partial detachment of the outer divertor[9]. Although this is in line with the observations at the HDL, this transport mechanism describes only the SOL plasma and does not explain how additional energy is ejected from the confined plasma.

At high densities, the fueling of the plasma changes, which leads to the non-linear density evolution. In the present work, this is considered to be an H-mode fueling limit, as introduced in Section II B. First, the density of the confined plasma saturates. The further density increase takes place only in the SOL, where an electron density plateau evolves between the separatrix and the limiter. In the third phase, the density does also not increase any more in the SOL.

The density plateau in the SOL might influence the fueling significantly. Measurements by the fast reciprocating probe in the SOL indicate that the measured density (see Fig. 10) consists of a background density and an averaged contribution by filaments. First simulations of the radial neutral density and ionization profiles with the KN1D code[17] indicate an outward shift of the ionization profile. This is in line with the observed fueling limit, i.e. the saturated density of the confined plasma, and evolution of the background density in the SOL. With the increased SOL density, the ionization profile is shifted even further outside and neutral particles might not penetrate the confined plasma any more.

Although we introduced two mechanisms, which potentially explain each of the two effects of the HDL, these mechanisms have to be coupled to each other. Otherwise, it is unlikely that both effects always start and end simultaneously, which leads to the sharp bends in the graphs of Figures 7 & 8. The coupling of the two mechanisms will be subject to future studies.

Comparison between full-C and full-W AUG

The four phases are also observed in the full-C AUG (see Fig. 8). This indicates, that also with carbon as a wall material, a combination of an energy loss channel and a fueling limit leads to the HDL.

However, for full-C AUG it is reported[5,6], that the full detachment causes the HDL. It is likely, that the change of the wall material lead to a change or modification of the energy loss mechanism, while keeping the according combination of fueling limit and energy loss channel. The full detachment of the divertor might occur at full-C AUG at lower densities than the energy loss channel observed for full-W AUG. The observed change in the parameter dependencies of the HDL for the different wall materials can also be assigned to a changed energy loss mechanism. A replacement of the energy loss channel might be attributed to the changed radiation characteristics of a carbon device, which also impacts the detachment behaviour. According to this, it might be possible to reproduce the behaviour of full-C AUG at full-W AUG with nitrogen seeding. However, this could not be tested as nitrogen seeding is not directly applicable in the HDL discharges at full-W AUG due to the requirements of the non-standard operation at the highest densities (see Sec. II B).

VII. EXCEEDING THE H-MODE DENSITY LIMIT WITH CENTRALLY ELEVATED DENSITY PROFILES

In present tokamaks, at high densities, the density profiles of gas puffed discharges are flat due to the high collisionality[2]. For flat profiles, the edge, core and line averaged density are inherently related to each other. Thus, the density limits (Greenwald limit and HDL), which are most likely determined by edge parameters, can be correlated with the line averaged density. With centrally elevated density profiles, it is possible to disentangle these densities.

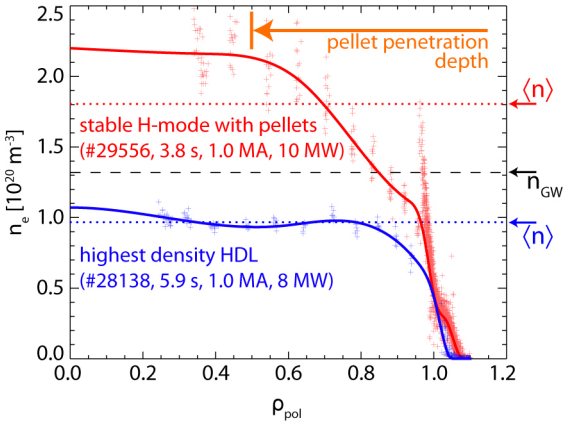

Figure 18. Density profiles of the HDL discharge with the highest density and a pellet fueled H-mode discharge. The central line averaged densities (H-1, dotted) and Greenwald density (dashed) are indicated.

At AUG, such centrally elevated density profiles can be achieved by pellet fueling[19]. In figure 18 the density profile of a gas puffed HDL discharge and a pellet fueled H-mode are compared. The gas puffed discharge exhibits a flat density profile and the line averaged density stays below the Greenwald density. With the pellet fueling, a centrally elevated density profile is achieved and the line averaged density exceeds the Greenwald density significantly, while the edge density stays well below the Greenwald density. The density gradient in the confined region ($\rho_{pol} < 0.95$) seems to be correlated to the radial range of the pellet particle source.

The energy confinement time τ_E stays constant for the pellet fueled discharge with and without pellets. The centrally increased density does not have an effect on the confinement, but the density dependence of the confinement scalings (e.g. ITERH98P(y,2)[27]) cannot be reproduced at these high densities[20].

Several experiments show that the Greenwald limit is determined to plasma edge parameters (e.g. JT-60[16], DIII-D[22], Tore Supra[10]). Also, H-modes with centrally elevated density profiles achieved Greenwald fractions above 1 (Fig. 18 or[20,22]), while keeping a moderate confinement. This suggests that both density limits, the Greenwald limit and the H-mode density limit, are correlated to the plasma parameters at and outside of the pedestal top ($\rho_{pol} \geq 0.95$).

Future tokamak fusion devices will operate with lower collisionality and, therefore, exhibit intrinsically peaked density profiles[1]. Consequently, it is possible that these tokamaks operate in a stable H-mode regime at Greenwald fractions above 1.

VIII. CONCLUSION

In gas ramp discharges performed at the fully tungsten covered ASDEX Upgrade tokamak, four discrete, quasi-stable plasma regimes are identified in the approach towards the H-mode density limit. These phases are distinguished by their impact on the plasma density and stored energy. They are identified as

- a **stable H-mode**, where the plasma density increases at a stable confinement,
- a **degrading H-mode**, where the confinement decreases while the density in the confined region stays constant and a plateau of electron density evolves in the SOL,
- the **breakdown of the H-mode**, where the overall radial density profile stays fixed while the confinement is decreasing and, finally,
- an **L-mode**, where the density increases again at almost constant, but low, confinement.

Several previously discussed mechanisms, such as the full detachment, increased radiation, MARFEs, and ELMs are refuted as a cause for the HDL in full-W AUG. Measurements indicate that a threshold of the depth of the radial electric field or of the power flux into the divertor, which aim to empirically describe the onset of the H-mode (either locally or globally), determines the final transition back to L-mode. However, both quantities are significantly above their thresholds at the onset of the HDL.

The observation of the four phases reveals, that an additional or increased energy loss channel must be present, which is seen in the decrease of stored energy in the second and third phase. This loss channel erodes the electron temperature gradient and the E_r well. Thus, the pedestal is deteriorated until the L-mode regime is reached. Along with this energy degradation the fueling of the plasma changes and a plateau of electron density evolves in the SOL. In particular, the overall density increase is interrupted at the third phase of the HDL until the pedestal is fully eroded. Both effects, the additional loss channel and the change of the plasma fueling, appear to be coupled to each other and their combination creates the four quasi-stable plasma regimes.

A promising candidate for the energy loss channel is a regime of increased radial filament transport in the SOL at high densities[9]. However, this model does not directly

explain the increased energy losses inside the separatrix. The density evolution and the related H-mode fueling limit might be connected to an outward shift of the ionization profile. Both effects are subject to further studies as the triggering and coupling mechanisms have to be identified.

With centrally elevated density profiles, e.g. by pellet fueling, it is possible to exceed the HDL and Greenwald limit scalings at a reasonable H-mode confinement[20]. This is strong evidence that both limits are determined by the plasma parameters at the pedestal top and further outside, as it is also indicated by the two proposed mechanisms of the HDL.

The latter finding might allow for future fusion power plants to operate in a stable H-mode regime at central densities above the Greenwald limit and, thus, increase the fusion power production. An identification of the mechanisms, which lead to the energy losses and the fueling limit, and their scaling to large scale devices is essential to find the optimal operational point for these machines with the highest attainable density and confinement.

ACKNOWLEDGMENTS

This project has received funding from the European Union's Horizon 2020 research and innovation program under grant agreement number 633053. The views and opinions expressed herein do not necessarily reflect those of the European Commission.

IX. REFERENCES

REFERENCES

[1]C. Angioni, E. Fable, M. Greenwald, M. Maslov, A. G. Peeters, H. Takenaga, and H. Weisen. Particle transport in tokamak plasmas, theory and experiment. *Plasma Physics and Controlled Fusion*, 51(12):124017, 2009.

[2]C. Angioni, R. M. McDermott, F. J. Casson, E. Fable, A. Bottino, R. Dux, R. Fischer, Y. Podoba, T. Pütterich, F. Ryter, and E. Viezzer. Intrinsic toroidal rotation, density peaking, and turbulence regimes in the core of tokamak plasmas. *Phys. Rev. Lett.*, 107:215003, Nov 2011.

[3]M. Bernert. *Analysis of the H-mode density limit in the ASDEX Upgrade tokamak using bolometry.* PhD thesis, LMU München, 2013.

[4]M. Bernert, T. Eich, A. Burckhart, J. C. Fuchs, L. Giannone, A. Kallenbach, R. M. McDermott, B. Sieglin, and the ASDEX Upgrade Team. Application of AXUV diode detectors at ASDEX Upgrade. *Review of Scientific Instruments*, 85(3):–, 2014.

[5]K. Borrass, J. Lingertat, and R. Schneider. A scrape-off layer based density limit for JET ELMy H-modes. *Contributions to Plasma Physics*, 38(1-2):130–135, 1998.

[6]K. Borrass, A. Loarte, C.F. Maggi, V. Mertens, P. Monier, R. Monk, J. Ongena, J. Rapp, G. Saibene, R. Sartori, J. Schweinzer, J. Stober, W. Suttrop, and the EFDA-JET Workprogramme collaborators. Recent H-mode density limit studies at JET. *Nuclear Fusion*, 44(7):752, 2004.

[7]K. Borrass, R. Schneider, and R. Farengo. A scrape-off layer based model for Hugill-Greenwald type density limits. *Nuclear Fusion*, 37(4):523, 1997.

[8]D. Carralero, G. Birkenmeier, H. W. Müller, P. Manz, P. de Marne, S. H. Müller, F. Reimold, U. Stroth, M. Wischmeier, E. Wolfrum, and the ASDEX Upgrade team. An experimental investigation on the high density transition of the scrape-off-layer transport in ASDEX Upgrade. submitted to Nucl. Fus.

[9]D. Carralero, H. W. Müller, M. Groth, M. Komm, J. Adamek, G. Birkenmeier, M. Brix, S. Marsen, C. Silva, U. Stroth, M. Wischmeier, E. Wolfrum, the ASDEX Upgrade Team, the COMPASS Team, and the JET-EFDA Contributors. Implications of high density operation on SOL transport: a multimachine investigation. submitted to Jour. Nucl. Mat.

[10]N. Commaux, A. Graud, B. Pgouri, F. Clairet, C. Gil, J. Gunn, G. Gros, E. Joffrin, and P. Hertout. Pellet fuelling experiments above the Greenwald density in Tore Supra. *Europhysics Conference Abstracts (Proc. of the 33rd EPS Conference on Controlled Fusion and Plasma Physics, Rome, 2006)*, 30I:P–5.105, 2006.

[11]L. Giannone, D. Queen, F. Hellman, and J. C. Fuchs. Prototype of a radiation hard resistive bolometer for ITER. *Plasma Physics and Controlled Fusion*, 47(12):2123, 2005.

[12]M. Greenwald. Density limits in toroidal plasmas. *Plasma Physics and Controlled Fusion*, 44(8):R27, 2002.

[13]M. Greenwald, J.L. Terry, S.M. Wolfe, S. Ejima, M.G. Bell, S.M. Kaye, and G.H. Neilson. A new look at density limits in tokamaks. *Nuclear Fusion*, 28(12):2199, 1988.

[14]A. Herrmann, T. Eich, V. Rohde, J. C. Fuchs, J. Neuhauser, and the ASDEX Upgrade team. Power deposition outside the divertor in ASDEX Upgrade. *Plasma Physics and Controlled Fusion*, 46(6):971, 2004.

[15]A. Huber, S. Brezinsek, M. Groth, P.C. de Vries, V. Riccardo, G. van Rooij, G. Sergienko, G. Arnoux, A. Boboc, P. Bilkova, G. Calabro, M. Clever, J.W. Coenen, M.N.A. Beurskens, T. Eich, S. Jachmich, M. Lehnen, E. Lerche, S. Marsen, G.F. Matthews, K. McCormick, A.G. Meigs, Ph. Mertens, V. Philipps, J. Rapp, U. Samm, M. Stamp, M. Wischmeier, and S. Wiesen. Impact of the ITER-like wall on divertor detachment and on the density limit in the JET tokamak. *Journal of Nuclear Materials*, 438, Supplement(0):S139 – S147, 2013. Proceedings of the 20th International Conference on Plasma-Surface Interactions in Controlled Fusion Devices.

[16]Y. Kamada, N. Hosogane, R. Yoshino, T. Hirayama, and T. Tsunematsu. Study of the density limit with pellet fuelling in JT-60. *Nuclear Fusion*, 31(10):1827, 1991.

[17]B. LaBombard. KN1D: A 1-D space, 2-D velocity, kinetic transport algorithm for atomic and molecular hydrogen in an ionizing plasma. Technical Report PSFC/RR-01-3, PSFC Report, MIT, Boston, USA, 2001.

[18]B. LaBombard, R. L. Boivin, M. Greenwald, J. Hughes, B. Lipschultz, D. Mossessian, C. S. Pitcher, J. L. Terry, S. J. Zweben, and the Alcator Group. Particle transport in the scrape-off layer and its relationship to discharge density limit in Alcator C-Mod. *Physics of Plasmas*, 8(5):2107–2117, 2001.

[19]P.T. Lang, A. Burckhart, M. Bernert, L. Casali, R. Fischer, O. Kardaun, G. Kocsis, M. Maraschek, A. Mlynek, B. Plöckl, M. Reich, F. Ryter, J. Schweinzer, B. Sieglin, W. Suttrop, T. Szepesi, G. Tardini, E. Wolfrum, D. Zasche, H. Zohm, and the ASDEX Upgrade Team. ELM pacing and high-density operation using pellet injection in the ASDEX Upgrade all-metal-wall tokamak. *Nuclear Fusion*, 54(8):083009, 2014.

[20]P.T. Lang, W. Suttrop, E. Belonohy, M. Bernert, R.M. McDermott, R. Fischer, J. Hobirk, O.J.W.F. Kardaun, G. Kocsis, B. Kurzan, M. Maraschek, P. de Marne, A. Mlynek, P.A. Schneider, J. Schweinzer, J. Stober, T. Szepesi, K. Thomsen, W. Treutterer, E. Wolfrum, and the ASDEX Upgrade Team. High-density H-mode operation by pellet injection and ELM mitigation with the new active in-vessel saddle coils in ASDEX Upgrade. *Nuclear Fusion*, 52(2):023017, 2012.

[21]B. Lipschultz, B. LaBombard, E.S. Marmar, M.M. Pickrell, J.L. Terry, R. Watterson, and S.M. Wolfe. Marfe: an edge plasma phenomenon. *Nuclear Fusion*, 24(8):977, 1984.

[22]M.A. Mahdavi, T.H. Osborne, A.W. Leonard, M.S. Chu, E.J. Doyle, M.E. Fenstermacher, G.R. McKee, G.M. Staebler, T.W. Petrie, M.R. Wade, S.L. Allen, J.A. Boedo, N.H. Brooks, R.J. Colchin, T.E. Evans, C.M. Greenfield, G.D. Porter, R.C. Isler, R.J. La Haye, C.J. Lasnier, R. Maingi, R.A. Moyer, M.J. Schaffer, P.G. Stangeby, J.G. Watkins, W.P. West, D.G. Whyte, and N.S. Wolf. High performance H mode plasmas at densities above the Greenwald limit. *Nuclear Fusion*, 42(1):52, 2002.

[23]Y. R. Martin, T. Takizuka, and the ITPA CDBM H-mode Threshold Database Working Group. Power requirement for accessing the H-mode in ITER. *Journal of Physics: Conference Series*, 123(1):012033, 2008.

[24]V. Mertens, K. Borrass, J. Gafert, M. Laux, J. Schweinzer, and the ASDEX Upgrade Team. Operational limits of ASDEX Upgrade H-mode discharges in the new closed divertor-II configuration. *Nuclear Fusion*, 40(11):1839, 2000.

[25]V. Mertens, M. Kaufmann, J. Neuhauser, J. Schweinzer, J. Stober, K. Buchl, O. Gruber, G. Haas, A. Herrmann, A. Kallenbach, and M. Weinlich. High density operation close to Greenwald limit and H-mode limit in ASDEX Upgrade. *Nuclear Fusion*, 37(11):1607, 1997.

[26]J. R. Myra, D. A. Russell, and D. A. D'Ippolito. Collisionality and magnetic geometry effects on tokamak edge turbulent transport. I. A two-region model with application to blobs. *Physics of Plasmas*, 13(11):112502, 2006.

[27]ITER Physics Expert Group on Confinement, Transport, ITER Physics Expert Group on Confinement Modelling, Database, and ITER Physics Basis Editors. Chapter2: Plasma confinement and transport. *Nuclear Fusion*, 39(12):2175, 1999.

[28]T. H. Osborne, J. R. Ferron, R. J. Groebner, L. L. Lao, A. W. Leonard, M. A. Mahdavi, R. Maingi, R. L. Miller, A. D. Turnbull, M. Wade, and J. Watkins. The effect of plasma shape on H-mode pedestal characteristics on DIII-D. *Plasma Physics and Controlled Fusion*, 42(5A):A175, 2000.

[29]S. Potzel, M. Wischmeier, M. Bernert, R. Dux, H.W. Müller, and A. Scarabosio. Characterization of the fluctuating detachment state in ASDEX Upgrade. *Journal of Nuclear Materials*, 438, Supplement(0):S285 – S290, 2013. Proceedings of the 20th International Conference on Plasma-Surface Interactions in Controlled Fusion Devices.

[30]F. Reimold, M. Wischmeier, M. Bernert, S. Potzel, A. Kallenbach, H. W. Müller, R. McDermott, M. Cavedon, B. Sieglin, A. Burckhart, G. Birkenmeier, R. Fischer, A. Scarabosio, and the ASDEX Upgrade Team. Divertor studies in nitrogen induced, completely detached H-modes in full-W ASDEX Upgrade. submitted to Nucl. Fus.

[31]G. Saibene, L.D. Horton, R. Sartori, B. Balet, S. Clement, G.D. Conway, J.G. Cordey, H.P.L. De Esch, L.C. Ingesson, J. Lingertat, R.D. Monk, V.V. Parail, R.J. Smith, A. Taroni, K. Thomsen, and M.G. von Hellermann. The influence of isotope mass, edge magnetic shear and input power on high density ELMy H modes in JET. *Nuclear Fusion*, 39(9):1133, 1999.

[32]P. Sauter, T. Pütterich, F. Ryter, E. Viezzer, E. Wolfrum, G.D. Conway, R. Fischer, B. Kurzan, R.M. McDermott, S.K. Rathgeber, and the ASDEX Upgrade Team. L- to H-mode transitions at low density in ASDEX Upgrade. *Nuclear Fusion*, 52(1):012001, 2012.

[33]J. Stober, O. Gruber, V. Mertens, F. Ryter, W. Suttrop, W. Treutterer, and the ASDEX Upgrade Team. Dependence of confinement and transport on triangularity in ASDEX Upgrade. *Europhysics Conference Abstracts (Proc. of the 26th EPS Conference on Controlled Fusion and Plasma Physics, Maastricht, 1999)*, 23J:1401–1404, 1999.

[34]W. Suttrop, V. Mertens, H. Murmann, J. Neuhauser, J. Schweinzer, and the ASDEX Upgrade Team. Operational limits for high edge density H-mode tokamak operation. *Journal of Nuclear Materials*, 266-269(0):118 – 123, 1999.

[35]E. Viezzer, T. Pütterich, G.D. Conway, R. Dux, T. Happel, J.C. Fuchs, R.M. McDermott, F. Ryter, B. Sieglin, W. Suttrop, M. Willensdorfer, E. Wolfrum, and the ASDEX Upgrade Team. High-accuracy characterization of the edge radial electric field at ASDEX Upgrade. *Nuclear Fusion*, 53(5):053005, 2013.

[36]E. Viezzer, T. Pütterich, R. Dux, R. M. McDermott, and the ASDEX Upgrade Team. High-resolution charge exchange measurements at ASDEX Upgrade. *Review of Scientific Instruments*, 83(10):103501, 2012.

[37]F. Wagner, G. Becker, K. Behringer, D. Campbell, A. Eberhagen, W. Engelhardt, G. Fussmann, O. Gehre, J. Gernhardt, G. v. Gierke, G. Haas, M. Huang, F. Karger, M. Keilhacker, O. Klüber, M. Kornherr, K. Lackner, G. Lisitano, G. G. Lister, H. M. Mayer, D. Meisel, E. R. Müller, H. Murmann, H. Niedermeyer, W. Poschenrieder, H. Rapp, and H. Röhr. Regime of improved confinement and high beta in neutral-beam-heated divertor discharges of the ASDEX tokamak. *Phys. Rev. Lett.*, 49(19):1408–1412, Nov 1982.

[38]H. Zohm. Edge localized modes (ELMs). *Plasma Physics and Controlled Fusion*, 38(2):105, 1996.